Tailoring Cellular Uptake of Gold Nanoparticles Via the Hydrophilic-to-Hydrophobic Ratio of their (Co)polymer Coating

Zhiyue Zhang, Katleen Van Steendam, Samarendra Maji, Lieve Balcaen, Yulia Anoshkina, Qilu Zhang, Glenn Vanluchene, Riet De Rycke, Frank Van Haecke, Dieter Deforce, Richard Hoogenboom, and Bruno G. De Geest**

It is demonstrated how cellular uptake and protein corona of (co)polymer-coated gold nanoparticles can be altered by the hydrophilic-to-hydrophobic comonomer ratio. A novel, label-free flow cytometry strategy is developed to investigate particle uptake. These findings offer insight in the design and analysis of hybrid nanomaterials for interfacing with biological systems.

1. Introduction

The design of engineered nanoparticles that can interact with living cells and tissues is important for many biomedical applications, including imaging, diagnostics, and drug delivery.[1] Gold nanoparticles (goldNP) have attracted major interest due to their chemical stability, cytocompatibility, and their tunable optical and electronic properties.[2] Furthermore, (quasi) covalent surface functionalization of metallic gold is straightforward using sulfur-containing compounds that form self-assembled monolayers.[3] Polymer-decoration of goldNP is attractive to modulate the goldNP properties and to render them colloidally stable in complex media. To produce polymer-decorated goldNP, reversible addition fragment chain-transfer polymerization (RAFT) is particularly well suited to synthesize sulfur-end-functionalized polymers due to the use of thiocarbonate RAFT chain transfer agents (CTAs).[4]

It is known that size, shape, and surface chemistry of goldNP affect their uptake by living cells.[5] However, few have been reported on whether altering the hydrophilic-to-hydrophobic ratio of a polymer coating can affect cellular interaction. In this paper we report on goldNP decorated with a series of polymers that differ in their hydrophilic-to-hydrophobic comonomer ratio and investigate how the latter affects cellular uptake. In addition, we developed a novel flow cytometry method for label-free investigation of goldNP-cell interaction. This methodology is then used to investigate the different parameters that affect the interaction of the goldNP and in vitro cultured cells.

Z. Zhang, Dr. K. Van Steendam, Prof. D. Deforce, Prof. B. De Geest
Department of Pharmaceutics
Ghent University
9000 Ghent, Belgium
E-mail: br.degeest@ugent.be

Dr. S. Maji, Dr. Q. Zhang, G. Vanluchene, Prof. R. Hoogenboom
Supramolecular Chemistry Group
Department of Organic and Macromolecular Chemistry
Ghent University
9000 Ghent, Belgium
E-mail: richard.hoogenboom@ugent.be

Dr. L. Balcaen, Y. Anoshkina, Prof. F. Van Haecke
Department of Analytical Chemistry
Ghent University
9000 Ghent, Belgium

R. De Rijcke
Department of Biomedical Molecular Biology
Ghent University
9000 Ghent, and Inflammation Research Center
VIB, 9052 Zwijnaarde, Belgium

DOI: 10.1002/adfm.201500904

2. Results and Discussion

Copolymers composed of the hydrophilic 2-hydroxyethylacrylate (HEA) and the hydrophobic methoxyethylacrylate (MEA) were obtained by RAFT in an automated parallel synthesis robot to minimize batch-to-batch variation.[6] Polymers with a theoretical degree of polymerization (DP; monomer to CTA ratio) of 100 and HEA:MEA ratios of 100:0, 80:20, 60:40, 50:50, 40:60, and 20:80, respectively, were synthesized according to **Scheme 1**. For clarity of presentation these polymers will further on be denoted as HEA_xMEA_y (x and y represent HEA and MEA to CTA ratio, respectively). Polymerization was stopped at a conversion of approximately 65% to ensure good chain end-fidelity of the polymers and Table S1, Supporting Information, summarizes their properties. In all cases linear first order polymerization kinetics (Figure S1, Supporting Information) were observed and good control over the polymerizations was further evidenced by dispersities below 1.3. As reported earlier by Hoogenboom et al., copolymers of HEA and MEA have an ideal random monomer distribution[7] which was confirmed in our present study. The polymers $HEA_{40}MEA_{60}$ and $HEA_{20}MEA_{80}$ appeared to by insoluble in water at room temperature or above and were not included in further experiments.

13 nm (size measured by transmission electron microscopy (TEM)) citrate-stabilized goldNP were synthesized by the

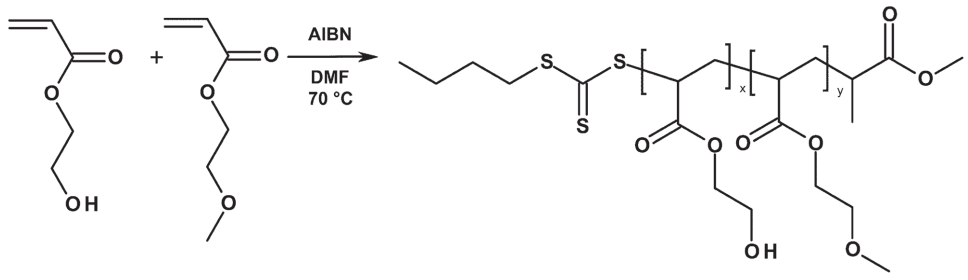

Scheme 1. Reaction scheme of the RAFT copolymerization of HEA and MEA.

Turkevich–Frens method via direct reduction of the $HAuCl_4$ salt with trisodium citrate in aqueous medium under boiling.[8] Characterization of the goldNP is reported in Figure S2-A, Supporting Information. Surface functionalization with the respective HEA_xMEA_y copolymers was performed by simply mixing aqueous solutions of the goldNP and copolymers (in large excess) followed by several centrifugation and washing steps to remove nonadsorbed polymer. Successful functionalization is evidenced by the ability of the polymer@goldNP solution to remain colloidally stable after removal of the access citrate. Indeed, when citrate-stabilized goldNP are centrifuged and redispersed in deionized water or buffer solution, irreversible aggregation occurs.[9] However, this was not the case in any of the HEA_xMEA_y@goldNP samples and dynamic light scattering (DLS) and TEM gave further proof of the formation of colloidally stable dispersions, as shown in Figure S2-B, Supporting Information. DLS and UV–vis further confirmed that the HEA_xMEA_y@goldNPs are stable at room temperature and at 37 °C in physiologically relevant media, including phosphate buffered saline (PBS; 50×10^{-3} M phosphate salts, 150×10^{-3} M NaCl, pH 7.4) and PBS supplemented with 10% fetal bovine serum (FBS; typically used in cell culture experiments and is composed of a complex mixture of serum proteins) (Figure S2-C and Table S2, Supporting Information).

The method of choice to measure cellular association (i.e., uptake or cell surface binding) of a specific component is flow cytometry (FCM). FCM involves the simultaneous measurements of light scattering and fluorescence properties of single cells as they move in a liquid stream through a laser/light beam past a sensing area. For this purpose, the components of interest are typically labeled with a fluorescent dye to allow, upon excitation by a laser beam, detection of fluorescence emission by a photomultiplier tube (PMT). Besides PMTs, flow cytometers are typically also equipped with diode detectors to measure scattered light in both axial (forward scatter; FSC) and perpendicular (side scatter; SSC) directions with respect to the fluid stream. The FSC signal is proportional to the cell size, whereas the SSC signal is proportional to the granularity of the cell. We hypothesized that cellular uptake of goldNP could, owing to the light scattering properties of goldNP, lead to an alteration in the SSC signal of the cells. If so and, this method would afford label-free detection of goldNP uptake by cells in a facile and high throughput fashion. Indeed, fluorescent labelling of a component of interest might significantly alter its physicochemical properties, and thus influence its interaction with cells. Additionally, metal nanoparticles are known to strongly quench fluorescence.[10] Thus, conjugating a fluorophore to the goldNP surface is very likely a suboptimal choice. Therefore, cellular uptake of goldNP is typically assessed by atomic absorption or emission spectroscopy. However, with regard to measuring metal content in cells, drawbacks of these methods include: 1) Careful sample preparation to know the exact cell number in each sample. 2) The nonhigh throughput nature of these techniques. 3) The impossibility to measure different parameters, as is the case with FCM using additional immunostains. 4) The lack of availability of these systems in common life sciences laboratories, whereas FCM is a well-established technique in this field.

As a proof-of-concept to validate whether indeed the SSC properties of cells change upon uptake of goldNP we incubated DC2.4 cells for 12 h with different concentrations of $HEA_{50}MEA_{50}$@goldNP. DC2.4 is an immortalized mouse dendritic cell (DC) line. DCs are the most potent class of professional antigen presenting cells of the immune system and a premier target cell population for the delivery of vaccine antigens and immune-modulating compounds. The FCM gating strategy that we applied to investigate the uptake of HEA_xMEA_y@goldNP in DC2.4 cells is shown in **Figure 1**A. Note that for the sake of clarity, these data correspond to blank untreated cells. The first two gates serve to discard multiplets (i.e., two or more cells that stick together) and cell debris. The two remaining cell populations marked by the red dashed ellipses represent dead cells (population (1)) and living cells (population (2)). We deliberately do not gate out the dead cell population based on the SSC versus FSC plot as is typically done in flow cytometry analysis. The reason for this is that as the SSC would increase upon internalization of goldNP, populations (1) and (2) would start to overlap. Thus, a priori gating out population (1) would mistakenly discard living cells that have internalized goldNP. Therefore, to gate out dead cells, we performed a costaining with propidium iodide (PI). This fluorescent dye is impermeable to alive cells but is permeable to dead cells and stains their nucleus. As a third gate, we selected those cells that were negative for PI staining. By counting the number of living cells per volume, we also verified that the concentration range of goldNP that was used in these experiments did not strongly affect cell viability (see Figure S3, Supporting Information). Finally, a gate was set to mark the onset of what will be considered as cells that are associated to goldNP (i.e., goldNP+ cells). As shown by the histograms in Figure 1B1, a shift in SSC can be clearly distinguished with increasing goldNP concentration in the cell culture medium. The quantitative results in Figure 1B2 give further proof that both the number of events in the goldNP+ cells gate and the

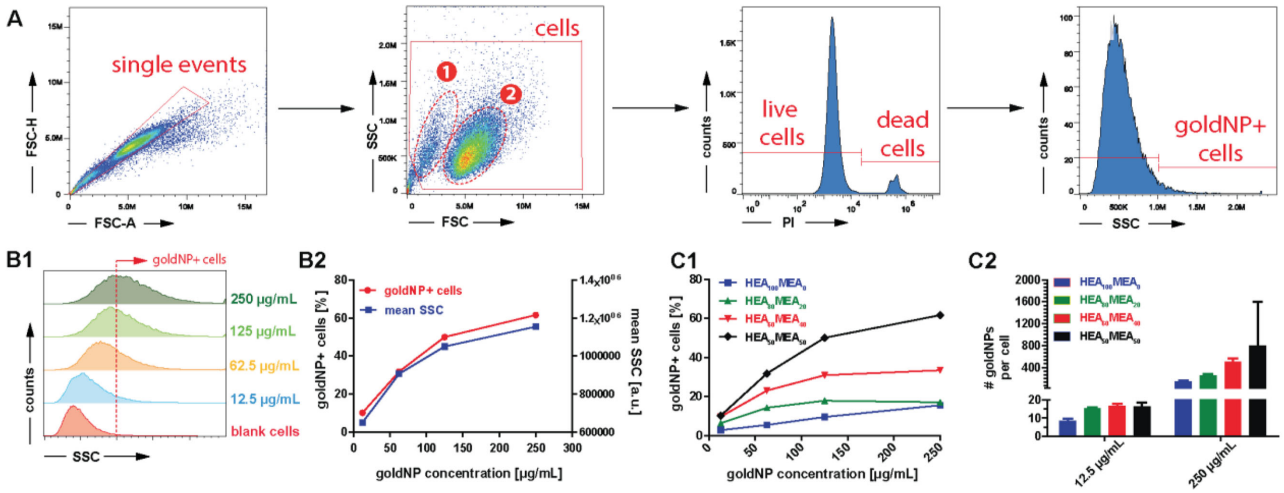

Figure 1. A) FCM gating strategy to assess cell uptake of goldNP by the shift in SSC. B) Histograms (B1) and quantitative analysis (B2) of DC2.4 cells pulsed with different concentrations of $HEA_{50}MEA_{50}$@goldNP ($n = 3$). C) Uptake HEA_xMEA_y@goldNP by DC2.4 cells measured by FCM (C1) and ICP-MS (C2) ($n = 3$).

mean SSC intensity in the living cells gate increase as a function of the goldNP concentration.

To enlarge our experimental setting, we incubated DC2.4 cells with increasing amounts of goldNP decorated with the different HEA_xMEA_y copolymers. As shown in Figure 1C1, a dose-dependent increase in SSC is witnessed for all HEA_xMEA_y@goldNP samples. Interestingly, also a strong influence of the hydrophilic-to-hydrophobic ratio of the polymer coating is observed, with increasing hydrophobicity of the polymer coating leading to increased goldNP-cell association. To validate our FCM strategy and to confirm whether the shift in SSC intensity as a function of goldNP concentration in the cell culture medium and polymer hydrophobicity is truly due to an increase in goldNP-cell association, we measured in parallel the goldNP content of the cells by inductive coupled mass spectroscopy (ICP-MS) for the lowest and highest goldNP concentrations in the cell culture medium. In these experiments we carefully assured that the number of cells in each sample was equal by counting cell numbers by FCM. As depicted in Figure 1C2, similar trends as observed by FCM are found, thereby confirming the high potential of this method for straightforward and high throughput screening of cellular interaction with goldNP.

To investigate whether the HEA_xMEA_y@goldNPs are effectively taken up by the DCs, or merely surface-bound, and to elucidate the intracellular fate of the nanoparticles, we used optical microscopy and TEM. The series of fluorescence microscopy images depicted in Figure S4, Supporting Information, indeed confirms the presence of nanoparticles observed as black dots inside the cells. Furthermore, DCs pulsed with $HEA_{100}MEA_0$@goldNP barely show presence of nanoparticles, whereas this is increasingly more pronounced for the other nanoparticle samples with increasing MEA content. This again confirms the FCM and ICP-MS data. Further insight into the intracellular localization of the goldNP was obtained by TEM on ultrathin microtomed sections taken from DCs that were pulsed with goldNP in a similar fashion as for the optical microscopy experiments. **Figure 2** shows that the nanoparticles are predominantly located inside vesicular organelles, likely endosomes, lysosomes, and/or phagosomes. Besides this, the zoomed images also show the presence of a minor fraction of the nanoparticles being localized outside vesicular organelles in the cytoplasm. No influence of the hydrophilic-to-hydrophobic ratio on the extent of cytoplasmic localization of the nanoparticles was observed. Although a minority, cytoplasm-located nanoparticles might play an important role. Indeed, as recently reported by Leong and coworkers, nanoparticles located in the cytosol can interfere with the microtubule assembly and, by doing so, strongly affect cellular migration capability.[11] Whether this is also the case for DCs, remains to be investigated. But in view of the crucial role of this highly motile nature of this cell type, a decrease in migratory properties could strongly affect the way DCs respond to an infectious tread or their ability to transport therapeutic nanoparticles (e.g., vaccines) to the immune-inducing sites in the draining lymph nodes.

Next we aimed at elucidating in more depth those parameters that play a role in the cellular internalization of the HEA_xMEA_y@goldNP. To investigate whether particle uptake proceeds via passive or active endocytosis, DC2.4 cells were incubated with the different HEA_xMEA_y@goldNP for 2 and 12 h at 37 and 4 °C, respectively. The latter is used to block active, energy-dependent, cell uptake. As shown in Figure S5, Supporting Information, a vast difference in particle uptake is observed dependent on the incubation time and temperature. First, after 2 h, the amount of goldNP+ cells is still fairly low relative to the values measured after 12 h. Second, incubation at 4 °C does not lead to significant particle uptake of any of the HEA_xMEA_y@goldNP samples, thereby suggesting that the cellular uptake of the particles proceeds via active receptor-mediated phagocytosis or macropinocytosis. This corresponds well with the TEM observations that show the nanoparticles being predominantly present in intracellular vesicles, which is a clear sign of an active uptake mechanism.[12]

When a nanomaterial enters a biological fluid (for example, cell culture medium), proteins rapidly absorb to its surface and, as a result, the surface properties, charges, and hydrodynamic

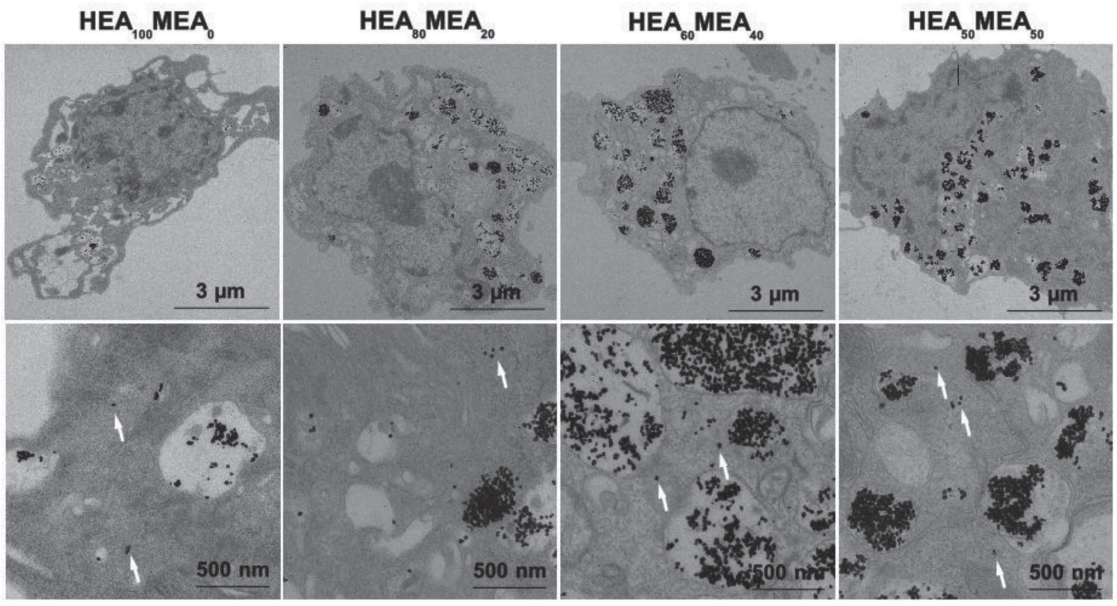

Figure 2. Transmission electron microscopy images at low (upper row) and high (lower row) zoom of DC2.4 cells incubated with HEA_xMEA_y@goldNP. Particles localized in the cytosol are marked by a white arrow.

radius of nanoparticles are reshaped.[13] The protein corona constitutes a primary nano–bio interface and determines the fate of nanoparticles in a biological environment. To investigate the role of serum proteins on the cellular uptake of the HEA_xMEA_y@goldNP, DC2.4 cells were pulsed for 2 h with the different HEA_xMEA_y@goldNP samples either in presence or absence of 10% FBS in the cell culture medium. Note that the 2 h time window was chosen because a period of 12 h in absence of serum was severely affecting cell viability. Depleting the cell culture medium from serum strongly reduces cellular association of all HEA_xMEA_y@goldNP samples. These findings suggest that the presence of serum plays an important role in governing cellular interaction with the HEA_xMEA_y@goldNP.[14]

The effect of the protein corona on the cellular uptake of the HEA_xMEA_y@goldNP was further elucidated by incubating the nanoparticles overnight in PBS supplemented with 10% FBS. Triple washing/centrifugation was used to remove the excess of proteins and the samples were subjected to an enzymatic digestions and analyzed by ζ-potential measurement and liquid chromatography combined with tandem mass spectrometry/mass spectrometry for detection (LC-MS/MS). The ζ-potential values of the respective nanoparticles are listed in Table S2, Supporting Information, and do not show major differences as a function of polymer coating before and after exposure to FBS. Therefore, it is likely that the ζ-potential values cannot be accounted for the differences in cellular interaction of the nanoparticles. Prior to LC-MS/MS analysis, the FBS-exposed HEA_xMEA_y@goldNP were loaded on polyacrylamide gel (PAGE) and subjected to electrophoresis followed by in-gel digestion with trypsin. Three biological replicates were analyzed per polymer. Quantification of the protein amount by optical integration of the PAGE gel (**Figure 3**A1) does show a higher amount of proteins absorbed to the HEA100 polymer. However, the difference was not significant.

Semi-quantitative analyses based on the number of identified proteins (Figure 3A2), and the number of spectra showed similar results. We also performed quartz crystal microbalance (QCM) studies on planar gold films on which HEA_xMEA_y polymers were adsorbed followed by flowing a PBS + 10% FBS solution over the chips. These experiments (Figure S6 and Table S3, Supporting Information) also did not indicate a difference in the absolute amount of proteins that are adsorbed onto the different HEA_xMEA_y coated chips, confirming the optical integration and LC-MS/MS data. These findings are contrary to earlier reports on planar gold surfaces[15] and goldNP functionalized with low M_w compound of varying hydrophobicity.[16] The Rotello group reported that hydrophobic goldNPs show a higher tendency in binding serum proteins, which in turn decrease their cellular uptake. This inhibition effect was attributed to the repulsive interaction between anionic bovine serum albumin (BSA) and negatively charged cell membrane.[17] However, differences in nanoparticle surface chemistry, cell type, culture protocol, and uptake pathway may account for this discrepancy.[18] For example, direct reaction between the HEA_xMEA_y chains hydrogen bonding with the hydroxyl groups or the methoxy groups,[14b] and the cell surface could contribute to the increase in cellular uptake.

When analyzing the exact content of the protein corona further in depth, clear differences between the respective HEA_xMEA_y@goldNP were found. To process the LC-MS/MS data, we selected those proteins that were found in all three biological replicates and clustered these as a function of their appearance in the respective HEA_xMEA_y@goldNP samples (Figure 3B1). These data show that of a total of 65 proteins, 32 proteins are found in each of the samples. Other proteins are found exclusively in one of the samples, or in discrete combinations. The 32 proteins that were found in all of the samples are presented in Figure 3B2 in a heat map, representing the relative abundances of these proteins based on spectra count. Spectral count is a label-free, semi-quantitative measure for proteins abundance. $HEA_{50}MEA_{50}$, $HEA_{60}MEA_{40}$, and $HEA_{80}MEA_{20}$

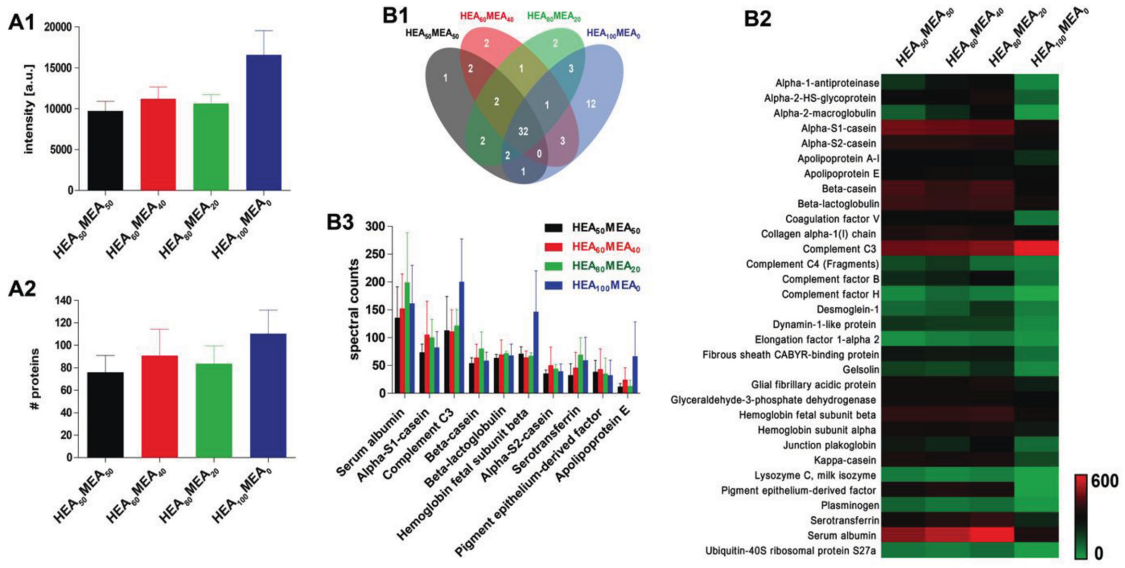

Figure 3. Proteomic analysis of HEA_xMEA_y@goldNP incubated in PBS + 10% FBS. A) Quantification of the total protein content by optical density integration (A1) of the PAGE gel and LC-MS analysis (A2). B) Finger printing of the protein corona. (B1) Schematic overview of the number of proteins that are found in the respective samples in all triplicate runs. (B2) Heat map of the relative abundance of the 32 proteins that were found in all triplicate runs in all HEA_xMEA_y samples. (B3) Spectral counts of the 10 most abundant proteins found in all triplicate runs in all HEA_xMEA_y samples ($n = 3$).

show similar results. $HEA_{100}MEA_0$, however, shows a discrepancy with the other polymers: some proteins are clearly upregulated in $HEA_{100}MEA_0$ such as Complement C3, others are downregulated such as alpha-S1-casein. Binding of complement C3 to hydroxyl bearing polymers (as is the case for HEA100) has been reported by the Hubbell group for purely organic nanoparticles[19] and is thus confirmed in our present studies for such polymers grafted on goldNP. Furthermore, the observation that $HEA_{100}MEA_0$ leads to the highest diversity of adsorbed proteins corresponds with earlier reports by the Whitesides group[20] that to avoid protein adsorption, a polymer should ideally have only hydrogen bond accepting groups and no hydrogen bond donating groups like $HEA_{100}MEA_0$ solely has. The full list of adsorbed proteins is included in the Supporting Information, and Figure 3B3 shows the spectral counts of the 10 most abundant proteins that were found in all HEA_xMEA_y@goldNP samples. GRAVY (grand average of hydropathy) analysis of the hydrophobicity of the absorbed proteins did not show difference in hydrophobicity of the absorbed proteins/peptides in function of the polymer coating. These observations suggest that either the subtle differences in the composition of the protein corona or the interaction between the polymer coating itself and the cell membrane might account for the increased particle uptake at increasing hydrophobicity of the polymer coating.

3. Conclusions

Summarizing, in this paper we have shown using a novel label-free FCM approach that tailoring the hydrophilic-to-hydrophobic ratio of the polymer coating of goldNP strongly influences cellular uptake. Serum proteins play a role in governing nanoparticle uptake, but its exact contribution needs to be further unraveled. Our current research efforts focus on investigation on the applicability of the FCM approach to measure cellular interaction with other crystalline and inorganic materials and its applicability to complex cell mixtures derived from live tissues. Furthermore, our findings can offer a rational base to design materials with varying cell interacting tendency, which might be useful for controlling residence time of nanoparticles in the blood stream or lymphatic vessels, both for therapeutic or research purpose.

4. Experimental Section

Materials: All chemicals were purchased from Sigma-Aldrich unless otherwise stated. Cell culture media and additives and AlexaFluor488-conjugated cholera toxin subunit B and propidium iodide were purchased from Life Technologies. The RAFT CTA (2-propanoicacid butyltrithiocarbonate (PABTC)) was synthesized according to literature.[21]

Synthesis of HEA_xMEA_y *Copolymers*: Stock solutions of 320 mg PABTC in 10.3 mL *N*,*N*-dimethylformamide (DMF), 22 mg azobisisobutyronitrile (AIBN) in 10.3 mL DMF, 7,80 g HEA in 9.08 mL DMF, and 8.75 g MEA in 8.16 mL DMF were prepared. The stock solution were de-oxygenized by bubbling through nitrogen for 30 min. In a ChemSpeed synthesis robot, each feed mixture was prepared twice, with feed ratios of 100/0, 80/20, 60/40, and 50/50 of HEA to MEA. To these mixtures were added 0.613 mL of PABTC stock solution and 0.613 mL of AIBN stock solution. Polymerizations were conducted at 70 °C under a nitrogen atmosphere while the liquid handling system was programmed to automatically take samples from the polymerization mixtures to follow the kinetics by gas chromatography (GC) and size exclusion chromatography (SEC). Based on the observed reaction kinetics, the polymerizations were repeated at a larger scale and the polymerizations were then stopped after 60 min by reducing temperature and bubbling with air. Polymers were then isolated by manual precipitation in a cold 50/50 mixture of diethyl ether and hexane.

Polymer Characterization: GC (Gas Chromatography): Gas chromatography was performed on a GC8000 from CE instruments with

a DB-5MS column (60 m × 0.249 mm × 0.25 m) from J&W scientific. Injections were performed with a CTC A200S auto sampler and detection was done with a flame ionization detector (FID) which burned a H2/air mixture. The carrier gas (He) was pushed through the column with a pressure of 100 bars. Injector and detector were kept at a constant temperature of 300 °C.

SEC (Size Exclusion Chromatography): Size-exclusion chromatography or gel permeation chromatography (GPC) was performed on a Agilent 1260-series HPLC system equipped with a 1260 online degasser, a 1260 ISO-pump, a 1260 automatic liquid sampler (ALS), a thermos tatted column compartment (TCC) at 50 °C equipped with two PLgel 5 m mixed-D columns in series, a 1260 diode array detector (DAD), and a 1260 refractive index detector (RID). The used eluent was DMA containing 50×10^{-3} M of LiCl at a flow rate of 0.593 mL min^{-1}. The spectra were analyzed using the Agilent Chemstation software with the GPC add on. Molar mass and polydispersity index (PDI) values were calculated against poly(methyl methacrylate) (PMMA) standards from polymer labs.

Cloud Point Temperature (T_{cp}) Measurement: Cloud point temperatures were determined on a Cary 300 Bio UV–visible spectrophotometer at a wavelength of 600 nm with a temperature controller. Aqueous polymer solution at 5 mg mL^{-1} were heated from 10 to 65 °C at a rate of 1 K min^{-1} followed by cooling to 10 at same rate of 1 °C min^{-1}. This cycle was repeated two times. The cloud point was reported as the 50% transmittance temperature in the heating run.

Synthesis of Citrate Stabilized goldNP: Citrate stabilized goldNP were synthesized according to literature.[8] All glassware was first washed with aqua regia and then rinsed with MilliQ water several times prior to synthesis. Briefly, 20 mL of an aqueous 1×10^{-3} M $HAuCl_4$ solution was refluxed for 30 min. Then 2 mL of 1 wt% sodium citrate solution was quickly added and the colour of solution changed from yellow to wine red within 5 min. After cooling, the reaction solution was stored at 4 °C until further use.

Polymer Functionalization of GoldNP: A total of 8 mL of a citrate stabilized gold nanoparticles solution was mixed with 200 mL of an aqueous solution containing 8 mg HEA_xMEA_y, and stirred overnight at room temperature. The polymer coated goldNP were purified three times by centrifugation at 4 °C with 15 000 g for 30 min followed by re-dispersion in MilliQ water.

Physicochemical Characterization of HEA_xMEA_y@goldNP: Transmission Electron Microscopy: Formvar/carbon-coated Cu grids (200-mesh) were used in all experiments. For TEM, A drop of gold nanoparticle solution was allowed to air-dry onto a grid, and was subsequently visualized using 80 keV TEM (Jeol 1010, Japan). TEM images of the goldNP were processed via Image J to determine the number average size distribution in dry state.

Dynamic Light Scattering: The size of particles (gold concentration of 0.18 mg mL^{-1}) was measured by DLS which was performed using a Malvern Zetasizer Nano Series running DTS software and operating a 4 mW He–Ne laser at 633 nm. Analysis was performed at an angle of 173°.

UV–Vis Spectroscopy: UV–vis spectra were acquired on a Shimadzu UV-1650PC spectrophotometer. In the case of temperature-dependent measurements, a Cary 300 Bio UV–visible spectrophotometer was utilized to check absorbance via changing the temperatures from 20 to 40 °C.

Cellular Uptake of HEA_xMEA_y@goldNP: The DC2.4 cell line is a kind gift from Dr. Ken Rock (Dana Farber Cancer Institute and presently University of Massachusetts Medical School).[22] DC2.4 cells were cultured in DMEM supplemented with 10% FBS and antibiotics (100 units per mL penicillin and 100 µg mL^{-1} streptomycin). Cells were grown at 37 °C in humidified air containing 5% CO_2 and passaged every 3–4 d. The cells were plated in a density of 250 000 per well (1 mL per well) on 24-well plates 24 h before addition of goldNP.

Flow Cytometry (FCM): All samples were measured on an Accuri (BD) flow cytometer and the data thus obtained were analyzed using FlowJo software.

Cell Viability Assay: DC2.4 cells were seed in 24-well plates at 250 000 cells per well in medium with 10% fetal bovine serum. After 24 h incubation, various concentrations of goldNP were added into cells. After another 12 h incubation, cell viability was measured by FCM via propidium iodide staining.

Effect of Incubation Temperature on GoldNP Cellular Uptake: DC2.4 cells were seeded in 24-well plates at 250 000 cells per well. After 24 h incubation, the cells were placed in fridge at 4 °C or in incubation culture at 37 °C for half an hour prior to pulsing with goldNP at varying concentrations. After another 12 h incubation, cells were washed with cold PBS and detached from the plates by adding 500 µL of ethylenediamine tetraaceticacid (EDTA) solution. Centrifugation at 300 g for 5 min was used to collect cells and then cells were treated with PI solution in PBS containing 1% BSA. After staining for 1 h at room temperature, the cells were measured via FCM.

Effect of Incubation Time on GoldNP Cellular Uptake: DC2.4 cells were seeded in 24-well plates at 250 000 cells per well. After 24 h incubation, cells were pulsed with goldNP at varying concentrations for another 2 or 12 h. cells were stained with PI solution prior to FCM analysis.

Effect of Serum Effect on GoldNP Cellular Uptake by DC2.4: DC2.4 cells were seeded in 24-well plates at 250 000 cells per well and cultured for 24 h at 37 °C in a medium with 10% fetal bovine serum. To investigate the serum effect in culture medium on goldNP cellular uptake, prior to addition of goldNP, cells were washed with PBS and exposed to a medium containing various concentrations of goldNP with and without serum. After another 2 h incubation, the cells were treated with PI and analyzed by FCM.

Fluorescence Microscopy: Fluorescence microscopy was performed on a Leica DM2500P microscope equipped with a 40× objective DC2.4 cells were plated a density of 15 000 per well in a 8-well Ibidi chamber and incubated overnight with 5 µL of a 2.50 mg mL^{-1} poly(HEA-MEA) coated goldNP suspension. AlexaFluor488 conjugated cholera toxin subunit B (cell membrane) and Hoechst (cell nuclei) staining was performed according to the manufactures' instructions.

Inductively Coupled Plasma-Mass Spectrometry (ICP-MS): ICP-MS was used to measure the amount of goldNP that were internalized by DC2.4 cells. DC2.4 cells were plated at a density of 250 000 cells per well and cultured for 24 h. Then cells were pulsed with different concentrations of goldNP. After 12 h incubation, cells were washed with PBS three times, detached from plates by EDTA, collected and digested with aqua regia on a hot plate (100 °C) for 10 h. After appropriate dilution of the digested samples, the concentration of gold was measured using ICP-MS (Element XR, ThermoScientific, Germany), and the average number of goldNP internalized by one cells was determined taking into account the size of the goldNP and the atomic weight of gold. The experiments were run in triplicate.

Transmission Electron Microscopy (TEM): Dendritic Cells from culture with HEA_xMEA_y@goldNP were fixed in 4% paraformaldehyde and 2.5% glutaraldehyde in 0.1 M NaCacodylate buffer, pH 7.2 and centrifuged at 500 rpm. Low melting point-agarose was used to keep the cells concentrated for the further processing. Cells were fixed for 4 h at RT followed by fixation O/N at 4 °C after replacing with fresh fixative. After washing in buffer, they were post fixed in 1% OsO4 with 1.5% K3Fe(CN)6 in 0.1 M NaCacodylate buffer at room temperature for 1 h. After washing, cells were subsequently dehydrated through a graded ethanol series, including a bulk staining with 1% uranyl acetate at the 50% ethanol step followed by embedding in Spurr's resin. Ultrathin sections of a gold interference color were cut using an ultramicrotome (Leica EM UC6), followed by a poststaining in a Leica EM AC20 for 40 min in uranyl acetate at 20 °C and for 10 min in lead stain at 20 °C. Sections were collected on formvar-coated copper slot grids. Grids were viewed with a JEM1010 transmission electron microscope (JEOL, Tokyo, Japan) operating at 80 kV using Image Plate Technology from Ditabis (Pforzheim, Germany).

Liquid Chromatography-Mass Spectrometry/Mass Spectrometry (LC-MS/MS): 500 µL of goldNP coupled to polymer were spun down (14 000 g, 4 °C, 10 min) and 400 µL of supernatant was removed. 24 µL of Laemmli buffer (50×10^{-3} M TrisHCl, pH 6.8, 2% SDS, 10% glycerol, bromophenol blue) and 12 µL of 500×10^{-3} M dithiotheitol (DTT) was added. Subsequently, the goldNP were heated to 70 °C for

1 h and centrifuged for 15 min, 14 000 g, 4 °C. 35 µL of supernatant was loaded on a 10% TrisHCl polyacrylamide gel (PAGE) and proteins were separated for 30 min at 150 V and 60 min at 200 V in running buffer (2.5×10^{-3} M Tris, 0.1% SDS, 192×10^{-3} M glycine). Proteins were visualized by Sypro Ruby staining (Invitrogen). Peak intensities were quantified by Quantity one software (Intxmm) (v4.1, Bio-Rad, Hercules, CA, USA). Extraction and digestion of the proteins was performed as previously described.[23] Dried peptides were dissolved in 0.1% formic acid (FA) in water (buffer A) and half of the sample was injected on reversed phase nanoHPLC column (Pepmap C18 column 15 cm, particle size 3 µm, 0.3 mm internal diameter by 150 mm; Dionex, Sunnyvale, CA, USA) using a linear gradient of 97:3 buffer A/bufferB to 20:80 buffer A/buffer B at 300 nL min^{-1} over 70 min (buffer B: 80% ACN/0.1% FA). The different peptides were analyzed on a TripleTOF 5600 (ABSciex, Framingham, MA, USA) in a data dependent mode. Data analysis was performed with Mascot Daemon (Matrix Science, London, UK) (peptide mass tolerance: 15 ppm; fragment mass tolerance: 0.3 Da; fixed modification: carbamidomethyl (C); variable modifications: carbamidomethyl (N-term), oxidation (M), deamidation (NQ); database: Bovine, 5984 entries). Hydrophobicity of the identified proteins and peptides were determined by means of GRAVY index.

Quartz Crystal Microbalance: QCM traces were recorded in a Gamry eQCM 10 M equipped with an ALS flow cell. 10 MHz gold coated quartz chips were used.

Supporting Information

Supporting Information is available from the Wiley Online Library or from the author.

Acknowledgements

Z.Z. and Q.Z. acknowledge the CSC and UGent-BOF for funding. S.M. is grateful to FWO for the Pegasus Marie Curie postdoctoral fellowship. B.G.D.G. and R.H. acknowledge the FWO for funding. Lenny Voorhaar, Yens Jackers, Sofie Vande Casteele, and Liesbeth Vossaert are acknowledged for technical assistance.

Received: March 6, 2015
Revised: April 8, 2015
Published online: May 13, 2015

[1] a) E. Boisselier, D. Astruc, *Chem. Soc. Rev.* **2009**, *38*, 1759; b) C. J. Murphy, A. M. Gole, J. W. Stone, P. N. Sisco, A. M. Alkilany, E. C. Goldsmith, S. C. Baxter, *Acc. Chem. Res.* **2008**, *41*, 1721; c) J. J. Storhoff, A. D. Lucas, V. Garimella, Y. P. Bao, U. R. Muller, *Nat. Biotechnol.* **2004**, *22*, 883; d) S. D. Brown, P. Nativo, J.-A. Smith, D. Stirling, P. R. Edwards, B. Venugopal, D. J. Flint, J. A. Plumb, D. Graham, N. J. Wheate, *J. Am. Chem. Soc.* **2010**, *132*, 4678; e) P. Ghosh, G. Han, M. De, C. K. Kim, V. M. Rotello, *Adv. Drug Delivery Rev.* **2008**, *60*, 1307; f) R. A. Sperling, P. Rivera gil, F. Zhang, M. Zanella, W. J. Parak, *Chem. Soc. Rev.* **2008**, *37*, 1896.

[2] a) M. C. Daniel, D. Astruc, *Chem. Rev.* **2004**, *104*, 293; b) D. N. Heo, D. H. Yang, H.-J. Moon, J. B. Lee, M. S. Bae, S. C. Lee, W. J. Lee, I.-C. Sun, I. K. Kwon, *Biomaterials* **2012**, *33*, 856; c) R. Elghanian, J. J. Storhoff, R. C. Mucic, R. L. Letsinger, C. A. Mirkin, *Science* **1997**, *277*, 1078; d) P. Zhang, T. K. Sham, *Phys. Rev. Lett.* **2003**, *90*, 245502.

[3] a) A. Badia, L. Demers, L. Dickinson, F. G. Morin, R. B. Lennox, L. Reven, *J. Am. Chem. Soc.* **1997**, *119*, 11104; b) J. C. Love, L. A. Estroff, J. K. Kriebel, R. G. Nuzzo, G. M. Whitesides, *Chem. Rev.* **2005**, *105*, 1103.

[4] P.-C. Chen, G. Shen, Y. Shi, H. Chen, C. Zhou, *ACS Nano* **2010**, *4*, 4403.

[5] a) W. Jiang, B. Y. S. Kim, J. T. Rutka, W. C. W. Chan, *Nat Nanotechnol.* **2008**, *3*, 145; b) B. D. Chithrani, A. A. Ghazani, W. C. W. Chan, *Nano Lett.* **2006**, *6*, 662; c) P. P. Pillai, S. Huda, B. Kowalczyk, B. A. Grzybowski, *J. Am. Chem. Soc.* **2013**, *135*, 6392; d) B. Kim, G. Han, B. J. Toley, C.-K. Kim, V. M. Rotello, N. S. Forbes, *Nat. Nanotechnol.* **2010**, *5*, 465; e) A. Verma, O. Uzun, Y. H. Hu, Y. Hu, H. S. Han, N. Watson, S. L. Chen, D. J. Irvine, F. Stellacci, *Nat. Mater.* **2008**, *7*, 588.

[6] a) C. R. Becer, A. M. Groth, R. Hoogenboom, R. M. Paulus, U. S. Schubert, *Qsar. Comb. Sci.* **2008**, *27*, 977; b) L. Voorhaar, S. Wallyn, F. E. Du Prez, R. Hoogenboom, *Polym. Chem.* **2014**, *5*, 4268.

[7] a) W. Steinhauer, R. Hoogenboom, H. Keul, M. Moeller, *Macromolecules* **2010**, *43*, 7041; b) R. Hoogenboom, A. M. Zorn, H. Keul, C. Barner-Kowollik, M. Moeller, *Polym. Chem.* **2012**, *3*, 335.

[8] a) J. Turkevich, P. C. Stevenson, J. Hillier, *Discuss. Faraday Soc.* **1951**, *11*, 21; b) G. Frens, *Nat. Phys. Sci.* **1973**, *241*, 3.

[9] Z. Zhang, S. Maji, A. B. d. F. Antunes, R. De Rycke, Q. Zhang, R. Hoogenboom, B. G. De Geest, *Chem. Mater.* **2013**, *25*, 4297.

[10] a) C.-C. You, O. R. Miranda, B. Gider, P. S. Ghosh, I.-B. Kim, B. Erdogan, S. A. Krovi, U. H. F. Bunz, V. M. Rotello, *Nat. Nanotechnol.* **2007**, *2*, 318; b) F. Li, H. Pei, L. Wang, J. Lu, J. Gao, B. Jiang, X. Zhao, C. Fan, *Adv. Funct. Mater.* **2013**, *23*, 4140; c) N. Kato, F. Caruso, *J. Phys. Chem. B* **2005**, *109*, 19604.

[11] C. Y. Tay, P. Cai, M. G. Setyawati, W. Fang, L. P. Tan, C. H. L. Hong, X. Chen, D. T. Leong, *Nano Lett.* **2014**, *14*, 83.

[12] I. Canton, G. Battaglia, *Chem. Soc. Rev.* **2012**, *41*, 2718.

[13] a) C. Y. Tay, M. I. Setyawati, J. Xie, W. J. Parak, D. T. Leong, *Adv. Funct. Mater.* **2014**, *24*, 5936; b) S. Tenzer, D. Docter, J. Kuharev, A. Musyanovych, V. Fetz, R. Hecht, F. Schlenk, D. Fischer, K. Kiouptsi, C. Reinhardt, K. Landfester, H. Schild, M. Maskos, S. K. Knauser, R. H. Stauber, *Nat. Nanotechnol.* **2013**, *8*, 772.

[14] a) T. Cedervall, I. Lynch, S. Lindman, T. Berggard, E. Thulin, H. Nilsson, K. A. Dawson, S. Linse, *Proc. Natl. Acad. Sci. U.S.A.* **2007**, *104*, 2050; b) C. D. Walkey, J. B. Olsen, H. Guo, A. Emili, W. C. W. Chan, *J. Am. Chem. Soc.* **2012**, *134*, 2139.

[15] K. L. Prime, G. M. Whitesides, *Science* **1991**, *252*, 1164.

[16] M. Lundqvist, J. Stigler, G. Elia, I. Lynch, T. Cedervall, K. A. Dawson, *Proc. Natl. Acad. Sci. U.S.A.* **2008**, *105*, 14265.

[17] Z.-J. Zhu, T. Posati, D. F. Moyano, R. Tang, B. Yan, R. W. Vachet, V. M. Rotello, *Small* **2012**, *8*, 2659.

[18] A. Albanese, W. C. W. Chan, *ACS Nano* **2011**, *5*, 5478.

[19] S. T. Reddy, A. J. van der Vlies, E. Simeoni, V. Angeli, G. J. Randolph, C. P. O'Neill, L. K. Lee, M. A. Swartz, J. A. Hubbell, *Nat. Biotechnol.* **2007**, *25*, 1159.

[20] R. G. Chapman, E. Ostuni, S. Takayama, R. E. Holmlin, L. Yan, G. M. Whitesides, *J. Am. Chem. Soc.* **2000**, *122*, 8303.

[21] Q. Zhang, N. Vanparijs, B. Louage, B. G. De Geest, R. Hoogenboom, *Polym. Chem.* **2014**, *5*, 1140.

[22] Z. H. Shen, G. Reznikoff, G. Dranoff, K. L. Rock, *J. Immunol.* **1997**, *158*, 2723.

[23] K. Van Steendam, K. Tilleman, M. De Ceuleneer, F. De Keyser, D. Elewaut, D. Deforce, *Arthritis Res. Ther.* **2010**, *12*, R132.